Chemical Engineering Journal 211–212 (2012) 360–368

Contents lists available at SciVerse ScienceDirect

Chemical Engineering Journal

journal homepage: www.elsevier.com/locate/cej

Kinetic modeling of arsenic (III) oxidation in water employing the UV/H_2O_2 process

Maia Lescano [a], Cristina Zalazar [a,b], Alberto Cassano [a,b], Rodolfo Brandi [a,b,*]

[a] INTEC (UNL-CONICET), Güemes 3450, 3000 Santa Fe, Argentina
[b] FICH (UNL), Ciudad Universitaria, Paraje El Pozo, 3000 Santa Fe, Argentina

HIGHLIGHTS

- A kinetic model for the oxidation of As (III) by the UV/H_2O_2 process is developed.
- The study includes dark and photoactivated reactions and estimates three parameters.
- A simplified model neglecting dark reactions is proposed.
- The kinetic models (complete and simplified) are in concordance with the experimental data.

GRAPHICAL ABSTRACT

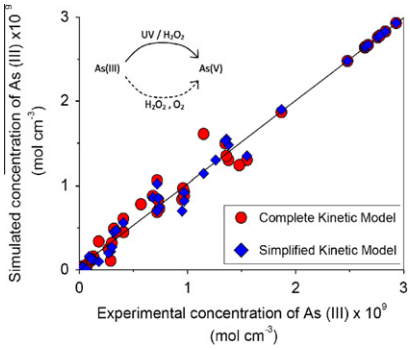

ARTICLE INFO

Article history:
Received 12 April 2012
Received in revised form 20 August 2012
Accepted 16 September 2012
Available online 5 October 2012

Keywords:
Arsenic oxidation
Kinetic modeling
UV/H_2O_2 process

ABSTRACT

In a previous study it has been shown that the combination of hydrogen peroxide and UVC radiation is an effective and feasible process to oxidize arsenic in water. In this work, a kinetic model for the photo-oxidation of As (III) is presented. An initial concentration of 200 μg/L of As (III) was used. The model was based on mechanistic reaction steps and included the modeling of the local radiation absorption effects. The evaluation of the radiation field inside the reactor was achieved by solving the radiative transfer equation for the homogeneous system. Both dark and photochemical arsenic oxidation rates were incorporated in the complete kinetic expression. Three parameters were estimated and a simplified model that only considered photoactivated reactions was developed. The rates obtained from these simplifications were compared with the rates from the complete model and showed a satisfactory concordance. The study was carried out in a cylindrical reactor operated in batch recirculation mode and two germicidal lamps were used (λ = 254 nm) as the source of radiation. Experimental runs were performed varying the hydrogen peroxide concentration and incident radiation. Both models rendered a good representation of the experimental data.

1. Introduction

The occurrence of dissolved arsenic in drinking water is a serious global problem. Groundwater contaminated by arsenic can have severe human health implications including various forms of cancer, cardiovascular and peripheral vascular disease and diabetes. Arsenic is released from soil into aquatic environment through natural processes (weathering of arsenic containing minerals) and anthropogenic activities (release of uncontrolled effluents from mining and metallurgical industries and use of organoarsenical pesticides) [1].

The chemical species of arsenic, which can exist in the natural environment, heavily influence its mobility, adsorption properties and toxicity [2]. In natural waters, arsenic may occur in both inorganic (As (III) and As (V)) and organic forms (monomethyl arsenic acid (MMAA) and dimethyl arsenic acid (DMAA)). Arsenite (As (III)) is the most toxic water-soluble species and arsenate (As (V)) is also relatively toxic. The methylated forms are much less toxic [3].

* Corresponding author at: INTEC (UNL-CONICET), Güemes 3450, 3000 Santa Fe, Argentina. Tel.: +54 342 4511370; fax: +54 342 4511087.
E-mail address: rbrandi@santafe-conicet.gov.ar (R. Brandi).

1385-8947/$ - see front matter © 2012 Elsevier B.V. All rights reserved.
http://dx.doi.org/10.1016/j.cej.2012.09.075

Nomenclature

C_i	concentration, mol cm^{-3}
C_i°	initial concentration, mol cm^{-3}
$e^a_{P,\lambda}$	local volumetric rate of photon absorption (LVRPA), Einstein cm^{-3} s^{-1}
$E^\lambda_{P,o}$	spectral fluence rate, Einstein cm^{-2} s^{-1}
$E^\lambda_{P,o,W}$	spectral fluence rate at the reactor windows, Einstein cm^{-2} s^{-1}
k_i	kinetic parameters, units depend on the reaction step
K_{27}	relation between k_2 and k_7 (k_2/k_7)
L_R	reactor length, cm
MSSA	micro-steady-state-approximation
Q	flow rate, cm^3 s^{-1}
r	molar concentration ratio
R_i^D	reaction rate for dark reaction, mol cm^{-3} s^{-1}
R_i^*	reaction rate for photoactivated reaction, mol cm^{-3} s^{-1}
t	time, s
V_R	photoreactor volume, cm^3
V_T	total system volume, cm^3
x	rectangular cartesian coordinate, cm

Greek letters

$\alpha_{\lambda,P}$	spectral linear naperian absorption coefficient of the hydrogen peroxide, cm^{-1}
Φ_P	primary quantum yield
$\kappa_{P,\lambda}$	molar naperian absorption coefficient, cm^2 mol^{-1}
λ	wavelength, nm

Special symbols

[]	concentration
$\langle\rangle$	averaged value over a defined space

Groundwater contains only inorganic forms of As (III) and As (V) [4].

Most technologies used for removing arsenic from water require the pre-oxidation of As (III) to As (V) to improve the removal of As (III) because As (V) adsorbs more strongly onto solid phase adsorbents than As (III) [5,6]. Arsenite can be oxidized with traditional oxidants (such as ozone, chlorine, permanganate, and hydrogen peroxide) [6–9] and advanced oxidation processes (AOPs) such as UV/TiO_2, UV/H_2O_2 [10–15]. These processes seem to be more efficient and convenient for the oxidation, because they do not generate toxic or undesirable by-products. The combination of UV light and H_2O_2 is an effective and feasible methodology for the oxidation of arsenic in water [16].

The kinetics of the oxidation of a wide range of organic pollutants employing the UV/H_2O_2 process has been extensively studied [17–22]. However, research on the mechanisms of oxidation of inorganic pollutants (arsenic in particular) and its reaction kinetics using hydrogen peroxide and UV light is not frequently reported in the existing bibliography.

Most studies deal with As (III) oxidation under different working conditions and focus on the factors that influence the reaction rates [15,23], but little information is provided on kinetic modeling based on mechanistic steps and including UV absorption effects. Few studies have reported the oxidation of arsenic by dissolved oxygen in water [9,24,25] and the efficiency of hydrogen peroxide as a direct oxidative agent [6,26]. The influence of these dark reactions in the combined UV/H_2O_2 process is not well known.

In this work, using the experimental data obtained in a previous research, a complete mathematical model derived from a reaction scheme of the arsenic oxidation is presented [16]. The model describes the evolution of As (III) and H_2O_2 in a photochemical reactor (laboratory scale) which operates inside a recycling system. It also considers the study of dark reactions and their effects in the process. In order to obtain intrinsic kinetic parameters, the model involves the evaluation of the radiation field and the solution of the mass balance for the existing species. The parameters obtained by this way provide a reliable intrinsic reaction kinetic. The aim of this research is to develop a kinetic model, as it is essential for design, process optimization and scaling up purposes.

2. Experimental

2.1. Reagents

The chemicals were of reagent grade. Sodium arsenite ($\geqslant$99%, Sigma–Aldrich p.a.) and hydrogen peroxide (30% w/v, Ciccarelli p.a) were used as the sources of As (III) and H_2O_2 respectively. As (III) and H_2O_2 solutions were accurately prepared daily to the required diluted concentrations. Fluka Catalase from bovine liver (2195 units/mg) was used. Ultra pure water (0.055 μS/cm) was employed for all dilutions.

2.2. Equipment and operating conditions

The reactor was a Teflon® cylinder closed with two flat, circular quartz windows inside of a recycling system (Fig. 1). The reactor length was 5.2 cm and the inner diameter was 5.2 cm (reactor volume = 110 cm^3). Irradiation was produced by two tubular Heraeus UV germicidal lamps, with one single significant emission wavelength at 253.7 nm, placed at the focal axis of their respective parabolic reflectors. Two optical neutral filters were used to carry out the experiments at different irradiation rates. They only permitted the transmission of 18% and 43% of the originally received spectral fluence rate. Each window allowed the placement of a shutter (a piece of flat metal) to block the light when necessary. The reactor was part of a recycling batch system that included: a large glass tank (2000 cm^3) with strong mechanical stirring and provisions for sampling and pH control and an all glass and Teflon® centrifugal recirculation pump (QVF ST 16 3 HS). The reactor was operated at a high recirculation flow rate, thus good mixing in the reactor was achieved (Q = 50 cm^3 s^{-1}). The circuit also included a refrigerating system to keep a constant temperature (20 °C).

Experiments were performed varying the concentration of hydrogen peroxide (between 0 and 30 mg/L) and the spectral fluence rate at the reactor windows ($E^\lambda_{P,o,W}$) (0, 1.4×10^{-9} and 22.4×10^{-9} Einstein cm^{-2} s^{-1}) at the same pollutant initial concentration (200 μg/L of As (III)). The values of dissolved oxygen was measured and ranged from 8.5 to 8.7 mg/L for all the experiments.

Table 1 details the operating conditions.

Each run was performed as follows: the germicidal lamps were turned on, allowing for 30 min for stabilizing their operation while the shutters were on. Then, the working solution was added to the reactor and the recirculation was established. When temperature was constant, the shutters were removed and the reaction started indicating the time t = 0. The objective was to reach the thermal and electrical stability of the system before the reaction began. The sampling (25 mL) was made at regular time intervals. After every run, the equipment was carefully washed. Due to the type of the equipment used in this work (a recycle with a tank) the total reaction time does not represent the time corresponding to the irradiation time of the reaction volume where the most important

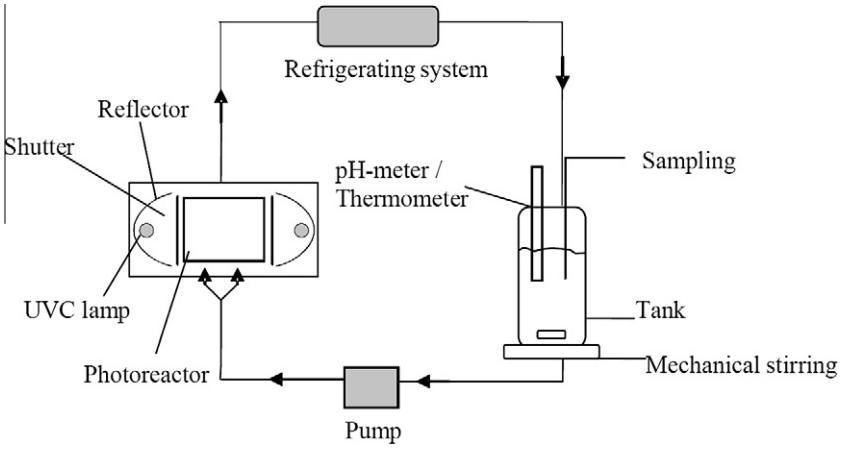

Fig. 1. Experimental setup.

Table 1
Experimental conditions.

Variable and units	Value
Arsenic (III) initial concentration (μg/L)	200
Hydrogen peroxide initial concentration (mg/L)	0–30
Spectral fluence rate at the reactor windows: $E^{\lambda=253.7\ nm}_{P,o,W}$ (einstein $cm^{-2}\ s^{-1}$) × 10^9:	
Heraeus 40 W lamp (100%)	22.4
Heraeus 40 W lamp (with filter) (43%)	9.8
Heraeus 40 W lamp (with filter) (18%)	4.1
Dissolved oxygen (mg/L)	8.5–8.7
Reaction time (min)	5, 15, 30
Initial pH	5.6–6.7
Temperature (°C)	20

reactions occur. Thus, for the actual exposure to radiation, the ratio given by the photoreactor volume over the total volume (V_R/V_T = 0.055) must be taken into account. More details can be found in [16].

2.3. Analysis

The arsenic concentration was measured using a Pekin Elmer AAnalyst 800 atomic absorption spectrometer (ASS). Each analysis was repeated three times to obtain the average value and the relative standard deviation (%RSD). The RSD value of the three replicate samples of each analysis was below 2.5%. Immediately after sampling, prior to the analysis of arsenic by ASS, a catalase solution was added to each sample in order to decompose the remaining hydrogen peroxide and avoid further oxidation.

For the arsenic speciation analyses, the samples were allowed to pass trough silica based strong anion exchange cartridges (SAX) with bonded group aminopropyl chloride form (Varian). The concentration of As (V) was calculated from the difference between the total arsenic concentration (before passing the cartridges) and the concentration of As (III) obtained by ASS.

The H_2O_2 concentration was analyzed by spectrophotometric method at 350 nm according to [27] and employing a Cary 100 Bio UV–visible instrument (the standard deviation value ranged from 0.05 to 0.08 for the calibration range studied). pH was controlled by HI 98127 Hanna pH meter (accuracy: ±0.1).

The spectral fluence rate at the reactor windows was experimentally measured by ferrioxalate actinometry according to [28,29].

Dissolved oxygen was measured by an Orion 830A meter.

3. Kinetic model

3.1. Reaction scheme

In the previous work, a reaction scheme for the oxidation of As (III) was developed [16]. However, some reactions and participating species have been slightly modified in order to improve the reaction mechanism. The reaction steps are summarized in Table 2. Photoactivated reactions involve reaction (1) and also the reactions generated from this UV absorption step (reactions (2)–(9)). Reactions (10) and (11) represent reaction steps which occur only in the dark.

It is widely accepted that the main interactions between hydrogen peroxide with UV light and free radicals are well represented by reactions (1)–(6) and their kinetic constants are well known [30,31]. Reactions (7) and (8) correspond to the oxidation of As (III) to the unstable As (IV) by the generated free radicals ($OH^{\cdot}$ and $HO_2^{\cdot}$). The resulting As (IV) can be oxidized with dissolved oxygen forming As (V) (reaction (9)).

Reactions (10) and (11) correspond to the direct oxidation of As (III) to As (V) by hydrogen peroxide and the presence of dissolved O_2 respectively. The significance of these reactions is discussed further in the corresponding section.

3.2. Kinetic equations

According to the experimental results and references from the bibliography, some assumptions were made in order to develop the kinetic model: (i) reactions 3, 4, and 6 will be neglected according to [19,32]; (ii) since the main oxidant species is the OH radical and superoxides have a less significant contribution to the main

Table 2
Reaction scheme.

No	Constants	Reactions
(1)	Φ_P	$H_2O_2 \rightarrow 2OH^{\cdot}$
(2)	k_2	$H_2O_2 + OH^{\cdot} \rightarrow HO_2^{\cdot} + H_2O$
(3)	k_3	$H_2O_2 + HO_2^{\cdot} \rightarrow OH^{\cdot} + H_2O + O_2$
(4)	k_4	$2OH^{\cdot} \rightarrow H_2O_2$
(5)	k_5	$2HO_2^{\cdot} \rightarrow H_2O_2 + O_2$
(6)	k_6	$OH^{\cdot} + HO_2^{\cdot} \rightarrow H_2O + O_2$
(7)	k_7	$H_3AsO_3 + OH^{\cdot} \rightarrow HAsO_3^{\cdot-} + H^+ + H_2O$
(8)	k_8	$H_3AsO_3 + HO_2^{\cdot} \rightarrow HAsO_3^{\cdot-} + HO_2^- + 2H^+$
(9)	k_9	$HAsO_3^{\cdot-} + O_2 + H_2O \rightarrow H_2AsO_4^- + HO_2^{\cdot}$
(10)	k_{10}	$H_3AsO_3 + H_2O_2 \rightarrow H_2AsO_4^- + H^+ + H_2O$
(11)	k_{11}	$H_3AsO_3 + O_2 + H_2O \rightarrow H_2AsO_4^- + H^+ + H_2O_2$

transformation, reaction (8) will be neglected [11]; (iii) k_2 was taken from the existing information [30]; (iv) the value of Φ_p (0.5) was taken from bibliography [31]; and (v) the micro-steady state approximation (MSSA) can be applied for highly reactive intermediates such as OH·, $HO_2^{\cdot}$ and $HAsO_3^{\cdot-}$ radicals. The model also assumes that H_2O and O_2 are in large excess over the other reactants; consequently, their concentrations are included in the constants k_9 and k_{11}, which provides two new pseudo kinetic constants k_{9g} and k_{11g} respectively [33,34].

3.2.1. Dark reaction rates

The reaction steps 10 and 11 of the reaction scheme represent the arsenic oxidation produced only by hydrogen peroxide and dissolved oxygen respectively (dark reactions). The reaction rates for the reactants can be written as follows:

For As (III)

$$R^D_{As(III)} = -k_{10}C_P C_{As(III)} - k_{11g}C_{As(III)} \quad (1)$$

For hydrogen peroxide

$$R^D_P = -k_{10}C_P C_{As(III)} + k_{11g}C_{As(III)} \quad (2)$$

3.2.2. Photoactivated reaction rates

According to the reaction scheme, the reaction rates for the reactants in photoactivated reactions can be written as follows:

For As (III)

$$R^*_{As(III)} = -k_7 C_{OH\cdot} C_{As(III)} \quad (3)$$

For hydrogen peroxide

$$R^*_P = -\Phi_p e^a_{P,\lambda} - k_2 C_P C_{OH\cdot} + k_5 C^2_{HO_2^{\cdot}} \quad (4)$$

For the case of the unstable intermediates OH·, $HO_2^{\cdot}$ and $HAsO_3^{\cdot-}$ resorting to the micro-steady-state-approximation (MSSA):

$$R^*_{OH\cdot} = 2\Phi_p e^a_{P,\lambda} - k_2 C_P C_{OH\cdot} - k_7 C_{OH\cdot} C_{As(III)} \cong 0 \quad (5)$$

$$R^*_{HO_2^{\cdot}} = k_2 C_P C_{OH\cdot} - 2k_5 C^2_{HO_2^{\cdot}} + k_{9g} C_{HAsO_3^{\cdot-}} \cong 0 \quad (6)$$

$$R^*_{HAsO_3^{\cdot-}} = k_7 C_{OH\cdot} C_{As(III)} - k_{9g} C_{HAsO_3^{\cdot-}} \cong 0 \quad (7)$$

From Eqs. (5)–(7):

$$C_{OH\cdot} = \frac{2\Phi_p e^a_{P,\lambda}}{(k_2 C_P + k_7 C_{As(III)})} \quad (8)$$

$$k_3 C^2_{HO_2^{\cdot}} = 0.5 k_2 C_P C_{OH\cdot} + 0.5 k_{9g} C_{HAsO_3^{\cdot-}} \quad (9)$$

$$k_{9g} C_{HAsO_3^{\cdot-}} = k_7 C_{OH\cdot} C_{As(III)} \quad (10)$$

Substituting Eq. (8) into Eq. (3) the reaction rate for As (III) results:

$$R^*_{As(III)} = \frac{-2\Phi_p e^a_{P,\lambda}}{\left(\frac{k_2 C_P}{k_7 C_{As(III)}} + 1\right)} \quad (11)$$

Substituting Eq. (10) into Eq. (9):

$$k_5 C^2_{HO_2^{\cdot}} = 0.5 k_2 C_P C_{OH\cdot} + 0.5 k_7 C_{OH\cdot} C_{As(III)} \quad (12)$$

Introducing Eq. (12) into Eq. (4) and resorting to Eq. (8) the reaction rate for hydrogen peroxide results:

$$R^*_P = -\Phi_p e^a_{P,\lambda} - \frac{\Phi_p e^a_{P,\lambda}}{\left(\frac{k_7 C_{As(III)}}{k_2 C_P} + 1\right)} + \frac{\Phi_p e^a_{P,\lambda}}{\left(\frac{k_2 C_P}{k_7 C_{As(III)}} + 1\right)} \quad (13)$$

Defining $r = C_P/C_{As\ (III)}$ as the molar ratio between hydrogen peroxide and arsenic and $K_{27} = k_2/k_7$, with some algebra we finally get the expressions of the reaction rates for the photoactivated reactions:

$$R^*_{As(III)} = \frac{-2\Phi_p e^a_{P,\lambda}}{(rK_{27} + 1)} \quad (14)$$

$$R^*_P = -\frac{2\Phi_p e^a_{P,\lambda}}{(rK_{27} + 1)} rK_{27} \quad (15)$$

The kinetic constant k_7 corresponds to the attack of the hydroxyl radical to As (III). k_2 corresponds to a photolysis step and its value was taken from a widely accepted reference [30] and Φ_p corresponds to the quantum yield and its value was taken from reference [31]. Since $C_{As\ (III)}$, C_p and LVRPA depend on position and time, the reaction rates for the photoactivated reactions represent local values that result in a function of position and time. A radiation balance is needed to calculate the LVRPA by H_2O_2.

Reaction rates expressions for dark and photoactivated reactions previously obtained were summarized in Table 3.

Table 3
Reaction rates.

Reactions	Reaction rates	
	Arsenic (III)	Hydrogen peroxide
Photoactivated	$R^*_{As(III)} = \frac{-2\Phi_p e^a_{P,\lambda}}{(rK_{27}+1)}$	$R^*_P = -\frac{-2\Phi_p e^a_{P,\lambda}}{(rK_{27}+1)} rK_{27}$
Dark	$R^D_{AS(III)} = -k_{10}C_P C_{AS(III)} + k_{11g}C_{As(III)}$	$R^D_P = -k_{10}C_P C_{AS(III)} + k_{11g}C_{As(III)}$

3.3. Radiation balance

The spectral LVRPA was calculated by solving the radiation balance in the experimental reactor. Alfano et al. [35–37] found that, for restricted optical and geometrical parameters, changes in the radial and angular coordinates did not introduce significant variations on the radiation field. Therefore, the radiation field in the system can be modeled by a one-dimensional representation. This simplification is useful because it renders simple equations that can be used for kinetic studies.

According to previous information and considering that only hydrogen peroxide absorbs radiation, the LVRPA at a given point in the reactor is given as follows [32]:

$$e^a_{P,\lambda}(x,t) = \alpha_{P,\lambda}(x,t) E^{\lambda}_{P,o}(x,t) \quad (16)$$

The spectral fluence rate at any point x inside the reactor is given by contributions of both lamp and reflectors. Thus,

$$E^{\lambda}_{P,o}(x,t) = E^{\lambda}_{P,o,W}\{\exp[-\alpha_{P,\lambda}(t)x] + \exp[-\alpha_{P,\lambda}(t)(L_R - x)]\} \quad (17)$$

Substituting Eq. (17) into Eq. (16):

$$e^a_{P,\lambda}(x,t) = \alpha_{P,\lambda} E^{\lambda}_{P,o,W}\{\exp[-\alpha_{P,\lambda}(t)x] + \exp[-\alpha_{P,\lambda}(t)(L_R - x)]\} \quad (18)$$

Since none species of As (III) absorbs at 253.7 nm, only H_2O_2 is involved in Eqs. (17) and (18). The value of the absorption coefficient was obtained by the direct application of Beers equations ($\alpha_{P,\lambda} = \kappa_{P,\lambda} C_P$), being $\kappa_{P,\lambda} = 0.389 \times 10^5 cm^2 mol^{-1}$. In order to compute the averaged value of LVRPA, the average integral was used:

$$\langle e^a_{P,\lambda}(x,t)\rangle_{V_R} = \frac{1}{L_R}\int_{L_R} e^a_{P,\lambda}(x,t)dx \quad (19)$$

According to (19), resorting to (18), the final expression used in this work is:

$$\langle e^a_{P,\lambda}(x,t)\rangle_{V_R} = \frac{2E^{\lambda}_{P,o,W}}{L_R}\{1 - \exp[-\alpha_{P,\lambda}(t)L_R]\} \quad (20)$$

This averaged value is needed because the LVRPA is an irreducible function of the spatial coordinates, i.e., there is not uniform distribution of the photons inside the reactor.

3.4. Mass balance

The mass balance of As (III) and H_2O_2 was solved in order to simulate the theoretical temporal changes of the pollutant and hydrogen peroxide.

Some simplifications were made: (i) there is a differential conversion per pass in the reactor, (ii) the system is perfectly mixed, (iii) the recirculation rate is very high (this operating condition is indispensable to ensure assumptions (i) and (ii)), (iv) photoactivated reactions occur only inside the reactor, and (v) dark reactions occur in the whole system. As a result, the concentration changes in the tank are related to the reaction rates as follows:

$$\left.\frac{dC_i(t)}{dt}\right|_{Tank} = \frac{V_R}{V_T}\langle R_i^*(x,t)\rangle_{V_R} + R_i^D(t) \tag{21}$$

With the initial condition that $C_i(t=0) = C_i^\circ$

3.5. Final expressions

The required volume averaged reaction rates for the mass balance can be obtained from the kinetic Eqs. (14) and (15) according to:

$$\langle R_i^*(x,t)\rangle_{L_R} = \frac{1}{L_R}\int_{L_R} R_i^*(x,t)dx \tag{22}$$

Substituting Eq. (20) and taking into account Eq. (21), we obtained a system of two ordinary differential equations:

$$\frac{dC_{As(III)}(t)}{dt} = -\frac{V_R}{V_T}\frac{2\Phi_p\langle e^a_{P,\lambda}\rangle}{(rK_{27}+1)} + R^D_{As(III)} \tag{23}$$

$$\frac{dC_P(t)}{dt} = -\frac{V_R}{V_T}\frac{2\Phi_p\langle e^a_{P,\lambda}\rangle}{(rK_{27}+1)}rK_{27} + R^D_P \tag{24}$$

Introducing Eqs. (1) and (2) into Eqs. (23) and (24), we finally obtain:

$$\frac{dC_{As(III)}(t)}{dt} = -\frac{V_R}{V_T}\frac{2\Phi_p\langle e^a_{P,\lambda}\rangle}{(rK_{27}+1)} - k_{10}C_{As(III)}C_P - k_{11g}C_{As(III)} \tag{25}$$

$$\frac{dC_P(t)}{dt} = -\frac{V_R}{V_T}\frac{2\Phi_p\langle e^a_{P,\lambda}\rangle}{(rK_{27}+1)}rK_{27} - k_{10}C_PC_{As(III)} + k_{11g}C_{As(III)} \tag{26}$$

The reacting system was studied under different operating conditions: (i) in absence of UV radiation and hydrogen peroxide (effect of dissolved O_2), (ii) in absence of UV radiation and addition of hydrogen peroxide, and (iii) employing the UV/H_2O_2 irradiated process. Different parameters were obtained from these conditions.

4. Results and discussion

4.1. Parameter estimation of dark reactions

4.1.1. In absence of UV radiation and H_2O_2

The experiment was performed employing an As (III) concentration of 200 μg/L. The initial pH was 6.5. According to the experimental data, an oxidation yield of 10% was reached after 30 min. This behavior could be explained by the effect of the dissolved oxygen. The dissolved oxygen was measured during the experience. The values ranged from 8.5 to 8.7 mg/L. The value of 8 mg/L corresponds to dissolved oxygen in water in equilibrium with air at room temperature. Kim and Nriagu [9] reported that oxidation of As (III) with dissolved air in water is possible though the efficiency of this process is very low. Other authors explained that the reaction may become important only if oxygen saturated water is used for the process [24,25]. Hence, even if the conversion is not very important in the oxidation of As (III) it must be part of the reaction mechanism. A rigorous evaluation and comparison of the most important reaction could show the possibility of neglecting dark reactions with no large error. Therefore, the constant k_{11g} should be evaluated in order to determine the influence of this reaction in the whole system:

Even if some amount of hydrogen peroxide is formed (see reaction step 11), it would be present at a very low concentration in the system. Therefore, in this case, the MSSA for the hydrogen peroxide can be applied and Eq. (25) results:

$$\frac{dC_{As(III)}(t)}{dt} = -2k_{11g}C_{As(III)} \tag{27}$$

Eq. (27) has an analytical solution. In order to obtain k_{11g}, the equation can be written as follows:

$$\ln\frac{C_{As(III)}}{C^\circ_{As(III)}} = -2k_{11g}t \tag{28}$$

The following kinetic constant was obtained from the experimental data and a simple linear regression:

$$k_{11g} = 2.08\times10^{-5} \pm 2.2\times10^{-6}\ s^{-1}$$

The reaction rate constant is very low. Nevertheless, the reaction occurs and it is important to include this parameter in a complete model to compare its magnitude with the other rate constants corresponding to H_2O_2 direct oxidation and UV/H_2O_2 photo oxidation.

Eary and Shramke [38] estimated a half-life of 360 days for the oxidation reaction of As (III) in groundwater by O_2. Kim and Nriagu [9], estimated half-lives of 4 min, 2–4 days, 4–9 days for the oxidation reaction of As (III) in groundwater under saturated conditions employing ozone, pure oxygen and air respectively.

In our case, the half-life for As (III) oxidation, according to the estimated parameter obtained was 9.3 h. The estimated value is different from the published values. This result could be probably explained by the different characteristics of the water employed (pH, presence of dissolved organic compounds, carbonates, phosphates, iron, cooper, etc.). In our case, the estimation was made employing solutions of As (III) in ultrapure water.

4.1.2. In absence of UV radiation and addition of H_2O_2

The runs were carried out employing an As (III) concentration of 200 μg/L and two different concentrations of H_2O_2 (3 mg/L, 4 mg/L). The initial pH for both experiments was 6.5.

According to the experimental data, oxidation yields reached 12% and 14.8% after 15 min, employing 3 and 4 mg/L of hydrogen peroxide respectively.

Once more, even if the conversions obtained are low in As (III) oxidation by H_2O_2, the effect of hydrogen peroxide should not be neglected as part of the reaction mechanism. It should be taken into account that if the reaction times were longer, the percentage of As (III) conversion would increase even more. The reason stated before for oxygen oxidation applies here. In the end, this reaction might not be really important. The direct oxidation of As (III) by direct hydrogen peroxide has been previously reported [6]. This publication explained that the reaction is strongly influenced by the existing pH, which gives rise to different dominant species that are thermodynamically feasible to undergoing oxidation. Thus, the constant k_{10}, as we said before, is influenced by the pH. Therefore, it is very important to estimate k_{10} value under the experimental conditions employed in this work in order to report the correct evaluation of the kinetic model that describes the UV/H_2O_2 process.

To determine the parameter k_{10}, Eqs. (25) and (26) result:

$$\frac{dC_{As(III)}(t)}{dt} = -k_{10}C_{As(III)}C_P - k_{11g}C_{As(III)} \quad (29)$$

$$\frac{dC_P(t)}{dt} = -k_{10}C_PC_{As(III)} + k_{11g}C_{As(III)} \quad (30)$$

Since there are not photons inside the system (LVRPA = 0), the terms involving $\Phi^a_{P,\lambda}$ and $\langle e^a_{P,\lambda}\rangle$ are deleted.

Eqs. (29) and (30) were solved by Runge–Kutta method. The kinetic constant k_{10} was obtained using the value of k_{11g} previously obtained, the experimental data and a non-linear least-squares (NLLSs) regression procedure based on Levenberg Marquardt optimization algorithm for parameter estimation. This procedure renders the values of the parameters that minimize the sum of squared differences between predicted concentrations from the model and experimental data.

$$k_{10} = 1.46 \times 10^3 \pm 9.70 \times 10^2 \text{ cm}^3 \text{ mol}^{-1} \text{ s}^{-1}$$

A comparison between the estimated kinetic parameter k_{10} and the published values for this reaction is presented in Table 4. It shows that the estimated value is a little lower than the published value measured at pH = 7.5. This result is reasonable according to the behavior of the rate constant as a function of the pH cited in reference [6]. It is reported that the rate constant involved in the direct oxidation of H_2O_2 to As (III) increases with the pH. Also, the values in the literature cited were determined from groundwater samples and, in our case, the values were determined employing solutions of As (III) in ultrapure water.

4.2. Parameter estimation for the complete process

The operating conditions employed for the parameter estimation for the complete process were:

(a) Concentration of As (III) = 200 μg/L; Concentration of H_2O_2 = 0.5 mg/L, 1, 2, 3, 6, 10, 15, 20, 30 mg/L; Spectral fluence rate at the reactor windows = 22.4×10^{-9} Einstein $\text{cm}^{-2}\,\text{s}^{-1}$.

(b) Concentration of As (III) = 200 μg/L; Concentration of H_2O_2 = 3 mg/L; Spectral fluence rate at the reactor windows = 9.8×10^{-9} Einstein $\text{cm}^{-2}\,\text{s}^{-1}$, 4.1×10^{-9} Einstein $\text{cm}^{-2}\,\text{s}^{-1}$.

The pH ranged from 5.6 to 6.7 for all the experiments.

To determine the kinetic constant K_{27} for the complete UV/H_2O_2 process, taking into account the parameters k_{10} and k_{11g} previously obtained, Eqs. (25) and (26) were solved by the Runge Kutta method. One additional kinetic constant with its corresponding 95% confidence interval was obtained using the kinetic model, the radiation balance, the mass balance and the experimental data resorting to the NLLSs regression procedure:

$$K_{27} = 1.11 \times 10^{-2} \pm 3.5 \times 10^{-3}$$

Since

$$k_2 = 2.7 \times 10^{10} \text{ mol}^{-1} \text{ cm}^3 \text{ s}^{-1}, \text{ then } k_7 = 2.42 \times 10^{12} \text{ mol}^{-1} \text{ cm}^3 \text{ s}^{-1}$$

Table 4
Estimated parameters for As (III) oxidation by H_2O_2 and published values.

Parameter	Estimated Value	Reference values [literature cited]
k_{10}($\text{mol}^{-1}\,\text{cm}^3\,\text{s}^{-1}$)	$1.46 \times 10^3 \pm 9.70 \times 10^2$ (pH = 6.5)	5.5×10^3, pH = 7.5 [6] 1.53×10^4, pH = 10 [6]

Table 5
Estimated parameter for As (III) oxidation (hydroxyl attack) and published values.

Parameter	Estimated value	Reference values [literature cited]
k_7($\text{mol}^{-1}\,\text{cm}^3\,\text{s}^{-1}$)	2.42×10^{12} (pH = 5.6–6.7)	1.8×10^{12}, pH = 1 [30] 1.0×10^{12}, pH = 1–3 [30] 9.0×10^{12}, pH = 10.6 [30]

A comparison between the parameter k_7 and the published values for this reaction is presented in Table 5. Apparently the kinetic constants are influenced by the pH because of the different As (III) species involved. The same behavior was observed for dark reactions. The estimated rate constant $k_7 = 2.42 \times 10^{12}$ $\text{mol}^{-1}\,\text{cm}^3\,\text{s}^{-1}$ and the published values are of the same order of magnitude. The value is similar but not the same because, as we said before, the kinetic parameter depends on the experimental conditions that were estimated and evaluated. The value is higher than the reference values which were estimated in acidic conditions, and lower than the estimated value at pH 10.6. This behavior is reasonable because of the pH employed in our experiments (the pH ranged from 5.6 to 6.7).

It is important to mention that the aim of this work is to determine a global constant K_{27} (k_2–k_7 relation). The constant k_2 was only used to obtain the value of k_7 and to evaluate and compare k_7 magnitude with the existing literature.

As an example, in Fig. 2a–f, model simulations and experimental results of As (III) and H_2O_2 concentrations as a function of time are compared for various hydrogen peroxide initial concentrations employing an initial As (III) concentration of 200 μg/L and 22.4×10^{-9} Einstein $\text{cm}^{-2}\,\text{s}^{-1}$ for the LVRPA.

The root mean square error (RMSE) based on the comparison of experimental results and simulated conversions from the model for As (III) and hydrogen peroxide was 7.8%.

The rather simple equations derived (the kinetic model) represent quite well the experimental data for the reactants As (III) and hydrogen peroxide. In addition to this, the model reproduces the behavior for different experimental conditions studied. Fig. 2e corresponds to an experiment carried out under the best operating conditions (H_2O_2 concentration is in the optimum range established in the previous work [16]). These conditions were a concentration of As (III) and H_2O_2 of 200 μg/L and 15 mg/L respectively. For higher relations, the As (III) conversion begins to decrease because of the scavenging effects of an excess of hydrogen peroxide on the OH radicals that are responsible for the oxidation reaction.

4.3. Simplified model

Taking into account that the experiments have shown low conversions of As (III) without UV light, it is possible to derivate a simplified model neglecting k_{10} and k_{11}. Eqs. (25) and (26) can be then written as:

$$\frac{dC_{As(III)}(t)}{dt} = -\frac{V_R}{V_T}\frac{2\Phi_p\langle e^a_{P,\lambda}\rangle}{(rK_{27}+1)} \quad (31)$$

$$\frac{dC_P(t)}{dt} = -\frac{V_R}{V_T}\frac{2\Phi_p\langle e^a_{P,\lambda}\rangle}{(rK_{27}+1)}rK_{27} \quad (32)$$

Employing the same methodology as discussed before, two one new kinetic parameter with its corresponding 95% confidence interval was obtained:

$$K_{27} = 9.6 \times 10^{-3} \pm 2.9 \times 10^{-3}$$

Since $k_2 = 2.7 \times 10^{10}$ $\text{mol}^{-1}\,\text{cm}^3\,\text{s}^{-1}$, then $k_7 = 2.8 \times 10^{12}$ $\text{mol}^{-1}\,\text{cm}^3\,\text{s}^{-1}$

The root mean square error (RMSE) based on the comparison of experimental results and simulated conversions from the model for As (III) and hydrogen peroxide was 7.9%.

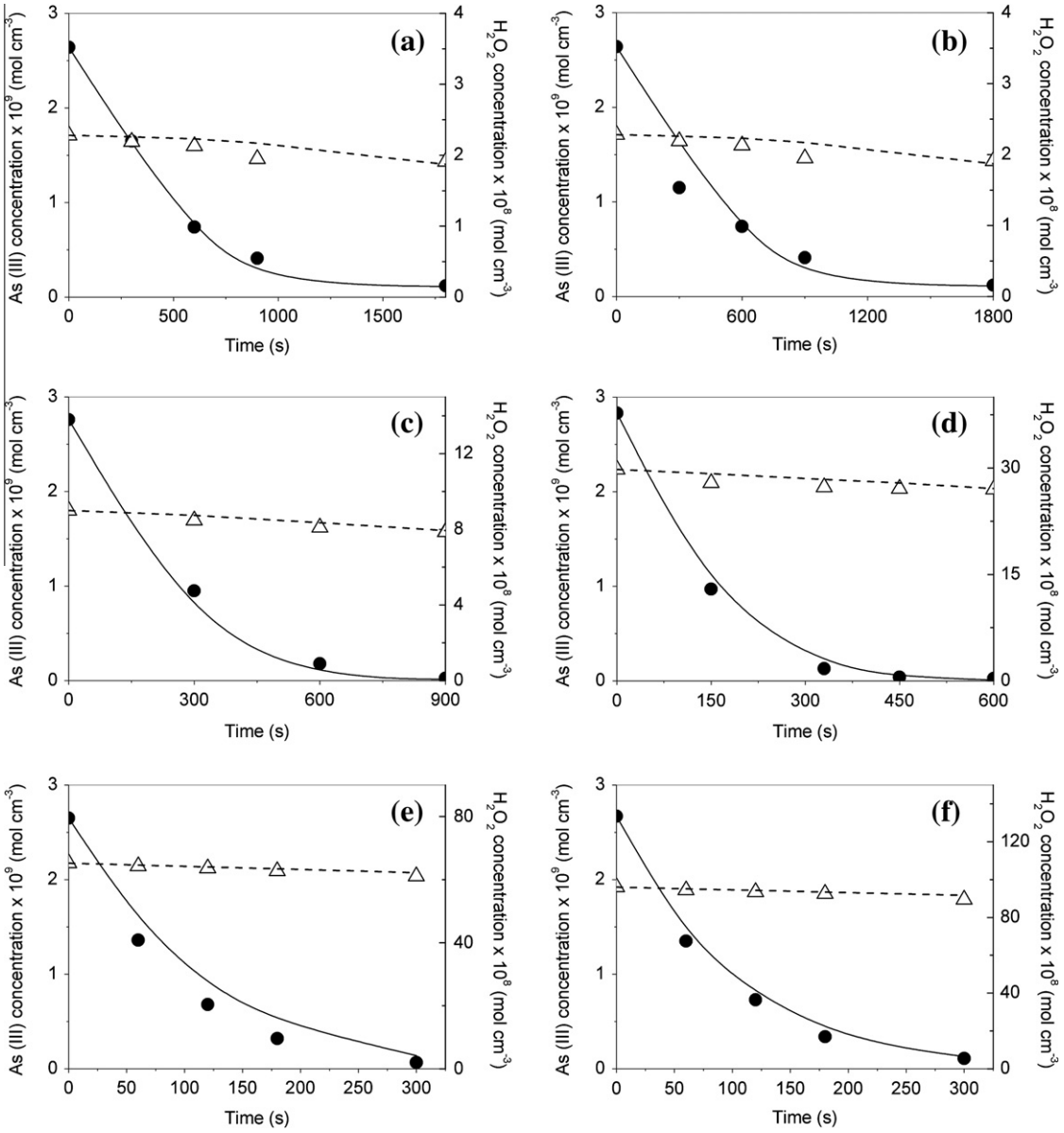

Fig. 2. Experimental and simulated concentrations of As (III) and H_2O_2 vs. time for different H_2O_2 initial concentrations. Experimental data: (●) As (III), (Δ) H_2O_2. Model simulation results: solid lines As (III), dash lines H_2O_2. (a) C_P = 1 mg/L; (b) C_P = 2 mg/L; (c) C_P = 3 mg/L; (d) C_P = 10 mg/L; (e) C_P = 20 mg/L; and (f) C_P = 30 mg/L. Initial concentration of As (III) = 200 μg/L; spectral fluence rate at the reactor windows = 22.4×10^{-9} Einstein cm^{-2} s^{-1}.

4.4. Comparison of the results obtained with the complete and the simplified models

A parity plot is useful to evaluate the model representation. The results obtained from the model and direct experimental data of As (III) and H_2O_2 concentrations for the complete and simplified models are compared in Figs. 3 and 4.

The distribution of the data around the parity line is a measure of the goodness of the proposed model. It can be seen that the model representation for hydrogen peroxide is good for both models (the R^2 values are >0.99). For As (III), the dots are a little more scattered about the parity line but they are distributed almost evenly on both sides of the straight line. For this pollutant, the representation of the proposed model is reasonable and the best R^2 is obtained for the simplified model.

It can be seen that both models (complete and simplified) represent the behavior of the involved species (experimental data) inside the reacting system.

The kinetic parameter k_7 obtained from the simplified model does not show significant differences with those obtained employing the complete scheme. According to these results, it is clear that the effects of the dark reactions could be neglected against the photoactivated reactions over the global reaction rate of the process. The constant k_7 involved in the attack of the hydroxyl radical to As (III) is relatively high, which assures the feasibility of the application of the UV/H_2O_2 process for the oxidation of As (III).

4.5. Feasibility and efficiency of the process

In order to evaluate its feasibility and efficiency, the process was compared with other technologies studied in the literature cited.

There are a lot of literature that presented the half-lives for As (III) employing 2 mg/L for the oxidant agent at pH 7.0: 16 h (H_2O_2) [6], 2 h (NH_2Cl) [7], 95 ms (HOCl) [7], 12 ms (O_3) [7] and 11 ms (FeO_4^{2-}) [39]. Also, Kocar and Inskeep [14] studied the As

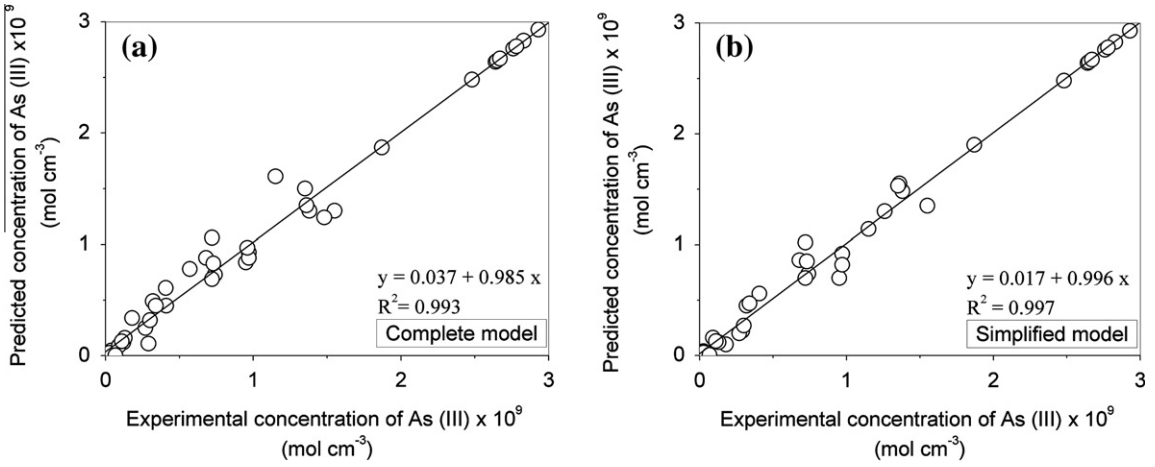

Fig. 3. Simulated concentrations of As (III) vs. experimental values. (a) Complete model. (b) Simplified model.

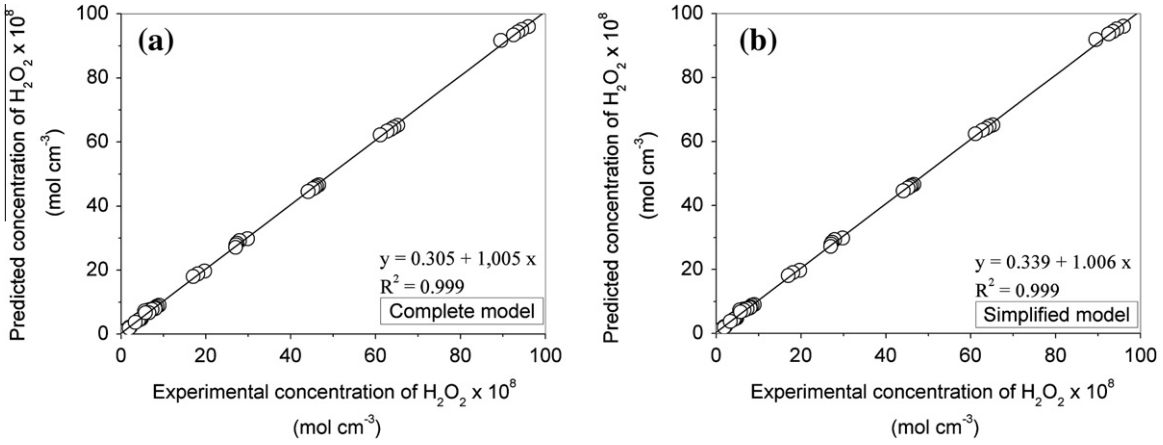

Fig. 4. Simulated concentrations of H_2O_2 vs. experimental values. (a) Complete model. (b) Simplified model.

(III) photochemical oxidation in presence of ferrioxalate in natural water, and obtained a half-life of 7.2 min (at pH 5.0 employing 18 μM of Fe (III) and 17.4 μM of As (III)). They compared this process with other technologies, employing values of half-lives for As (III) taken from this bibliography: O_2: 360 days [38]; Fe(III) at pH 5: 9.5 days [40]; H_2O_2 at pH 7.5: 1.6 days [6]; O_3: 4 min [9]; UV/TiO_2: 2.4 min [41]; biological processes: 0.6 min [42] and 18 min [43].

It can be seen from this review that it is very difficult to compare processes using experimental values obtained from different studies. It is because different conditions were employed in each study (different pH, different composition of the treated water, real groundwater samples, simulated groundwater samples, samples prepared with distilled water spiked with As (III), etc.). Nevertheless, the comparison could be useful in order to estimate and evaluate the relative feasibility and efficiency of a process.

In our study of the UV/H_2O_2 technology, from the experimental data or from the model (employing a concentration of H_2O_2 of 20 mg/L and a spectral fluence rate at the reactor windows of 22.4×10^{-9} Einstein $cm^{-2}\,s^{-1}$), a value of 3.5 s as a half-life for the As (III) oxidation process was obtained (pH: 6.6). Also, according to a previous publication from our group [16], the half-life obtained was 7.8 s for the same operating conditions but employing real groundwater samples.

According to the values of half-lives for As (III) summarized in this section, it can be concluded that even if the UV/H_2O_2 process is not as a fast as other processes that use oxidant agents (such as O_3, HOCl, and FeO_4^{2-}), it is fast in comparison with other oxidation advanced processes (photochemical oxidation in presence of ferrioxalate, UV/TiO_2, etc.) and biological processes.

5. Conclusions

A kinetic model for the oxidation of As (III) employing the UV/H_2O_2 process was developed.

The model involves dark and photoactivated reactions. They were studied separately and afterwards they were included as part of the whole system. By employing a simplified model, it has been demonstrated that the photoactivated reactions are the main responsible for the oxidation of As (III). Dark reactions have no significant influence on the overall reaction evolution.

The experimental data agreed with the data of the model predictions obtained from the proposed mechanism with a RMSE of 7.8% and 7.9% for the complete and simplified model respectively.

The process is relatively fast if it is compared with other oxidation processes studied. Therefore, it is a feasible and promising technique to be employed as a pre-oxidation treatment for As (III) contaminated water.

The results obtained in this work provide reliable intrinsic reaction kinetic parameters for reactor design and optimization purposes.

Acknowledgments

The authors are grateful to Universidad Nacional del Litoral (UNL), Consejo Nacional de Investigaciones Científicas y Técnicas (CONICET) and Agencia Nacional de Promoción Científica y Tecnológica (ANPCyT) for the financial support. They also thank Ing. Susana Gervasio for her valuable help in several steps of the analytical work.

References

[1] S. Yoon, K. Lee, S. Oh, J. Yang, Photochemical oxidation of As (III) by vacuum-UV lamp irradiation, Water Res. 42 (2008) 3455–3463.
[2] J. O'Reilly, M. Watts, R. Shaw, A. Marcilla, N. Ward, Arsenic contamination of natural waters in San Juan and La Pampa, Argentina, Environ. Geochem. Health 32 (2010) 491–515.
[3] Z. Li, S. Mou, Z. Ni, J. Riviello, Sequential determination of arsenite and arsenate by ion chromatography, Anal. Chim. Acta 307 (1995) 79–87.
[4] A. Chatterjee, D. Das, B. Mandal, T. Chowdhury, G. Samanta, D. Chakraborti, Arsenic in ground water in six districts of West Bengal, India: the biggest arsenic calamity in the world: Part I. Arsenic species in drinking water and urine of the affected people, Analyst 120 (1995) 643–650.
[5] J. Hug, O. Leupin, Iron-catalyzed oxidation of arsenic (III) by oxygen and by hydrogen peroxide: pH-dependent formation of oxidants in the Fenton reaction, Environ. Sci. Technol. 37 (2003) 2734–2742.
[6] M. Pettine, L. Campanella, F. Millero, Arsenite oxidation by H_2O_2 in aqueous solutions, Geochim. Cosmochim. Acta 63 (1999) 2727–2735.
[7] M. Dodd, N. Vu, A. Ammann, V. Le, R. Kissner, H. Pham, T. Cao, M. Berg, U. Von Gunten, Kinetics and mechanistic aspects of As (III) oxidation by aqueous chlorine, chloramines and ozone: relevance to drinking water treatment, Environ. Sci. Technol. 40 (2006) 3285–3292.
[8] G. Lee, K. Song, J. Bae, Permanganate oxidation of As (III). Reaction stoichiometry and the characterization of the solid product, Geochim. Cosmochim. Acta 75 (2011) 4713–4727.
[9] M. Kim, J. Nriagu, Oxidation of arsenite in groundwater using ozone and oxygen, Sci. Total Environ. 247 (2001) 71–79.
[10] H. Lee, W. Choi, Photocatalytic oxidation of arsenite in TiO_2 suspension: kinetics and mechanism, Environ. Sci. Technol. 36 (2002). 3872-3872.
[11] S. Yoon., J. Lee, Oxidation mechanism of As (III) in the UV/TiO2 system: evidence for a direct hole oxidation mechanism, Environ. Sci. Technol. 39 (2005) 9695–9701.
[12] T. Nakajima, Y. Xu, Y. Mori, M. Kishita, H. Takanashi, S. Maeda, A. Ohki, Combined use of photocatalyst and adsorbent for the removal of inorganic arsenic (III) and organoarsenic compounds from aqueous media, J. Hazard. Mat. 120 (2005) 75–80.
[13] S. Yoon, S. Oh, J. Yang, J. Lee, M. Lee, S. Yu, D. Pak, TiO_2 photocatalytic oxidation mechanism of As (III), Environ. Sci. Technol. 43 (2009) 864–869.
[14] B. Kocar, W. Inskeep, Photochemical oxidation of As (III) in ferrioxalate solutions, Environ. Sci. Technol. 37 (2003) 1581–1588.
[15] S. Sorlini, F. Gialdini, M. Stefan, Arsenic oxidation by UV radiation combined with hydrogen peroxide, Water Sci. Technol. 61 (2010) 339–341.
[16] M. Lescano, C. Zalazar, A. Cassano, R. Brandi, Arsenic (III) oxidation of water applying a combination of hydrogen peroxide and UVC radiation, Photochem. Photobiol. Sci. 10 (2011) 1797–1803.
[17] M. Stefan, A. Hoy, J. Bolton, Kinetics and mechanism of the degradation and mineralization of acetone in dilute aqueous solution sensitized by the UV photolysis of hydrogen peroxide, Environ. Sci. Technol. 30 (1996) 2382–2390.
[18] J. Crittenden, S. Hu, D. Hand, S. Green, A Kinetic model for H_2O_2/UV process in completely mixed batch reactor, Water Res. 33 (1999) 2315–2328.
[19] C. Liao, M. Gurol, Chemical oxidation by photolytic decomposition of hydrogen peroxide, Environ. Sci. Technol. 29 (1995) 3007–3014.
[20] C. Sharpless, K. Linden, Experimental and model comparisons of cow- and medium-pressure Hg lamps for the direct and H_2O_2 assisted UV photodegradation of *N*-Nitrosodimethylamine in simulated drinking water, Environ. Sci. Technol. 37 (2003) 1933–1940.
[21] W. Song, V. Ravindran, M. Pirbazari, Process optimization using a kinetic model for the ultraviolet radiation-hydrogen peroxide decomposition of natural and synthetic organic compounds in groundwater, Chem. Eng. Sci. 63 (2008) 3249–3270.
[22] K. Li, M. Stefan, J. Crittenden, Trichloroethene degradation by UV/H_2O_2 advanced oxidation process: product study and kinetic modeling, Environ. Sci. Technol. 41 (2007) 1696–1703.
[23] H. Yang, W. Lin, K. Rajeshwar, Homogeneous and heterogeneous reactions involving As (III) and As (V) species in aqueous media, J. Photochem. Photobiol. A: Chem. 123 (1999) 137–143.
[24] D. Frank, D. Clifford, Arsenic (III) oxidation and removal from drinking water, US Environmental Protection Agency. EPA-600-52/86/021 (1986) 2–86.
[25] A. Bockelen, R. Niesner, Removal of arsenic in mineral water, Vom Hasser 78 (1992) 225–235.
[26] R. Molnár, E. Vircikova, P. Lech, Experimental study of As (III) by hydrogen peroxide, Hidrometallurgy 35 (1994) 1–9.
[27] A. Allen, C. Hochanadel, J. Ghormley, Descomposition of water and aqueous solutions under mixed fast neutron and gamma radiation, J. Phys. Chem. 56 (1952) 575–586.
[28] S. Murov, I. Carmichael, G Hug, Handbook of Photochemistry, second ed., New York, 1993.
[29] C. Zalazar, M. Labas, C. Martín, R. Brandi, O. Alfano, A. Cassano, The extended use of actinometry in the interpretation of photochemical reaction engineering data, Chem. Eng. J. 109 (2005) 67–81.
[30] G. Buxton, C. Greenstock, W. Helman, A. Ross, Critical review of data constants for reactions of hydrated electrons, hydrogen atoms and hydroxyl radicals in aqueous solutions, J. Phys. Chem. Ref. Data 17 (1988) 513–886.
[31] P. Maruthamuthu, S. Padmaja, R. Huie, Rate constants for some reactions of free radicals with haloacetates in aqueous solution, Int. J. Chem. Kinet. 27 (1995) 605–612.
[32] C. Zalazar, M. Lovato, R. Brandi, A. Cassano, Intrinsic kinetics of the oxidative reaction of Dichloroacetic acid degradation employing hydrogen peroxide and UV radiation, Chem. Eng. Sci. 62 (2007) 5840–5853.
[33] J. Moore, R. Pearson, Kinetics and Mechanism, third ed., John Wiley & Sons, New York, 1981.
[34] M. Boudart, Kinetics of Chemical Processes, Prentice-Hall, New Jersey, 1968.
[35] O. Alfano, R. Romero, A. Cassano, A cylindrical photoreactor irradiated from the bottom-I. Radiation flux density generated by a tubular source and a parabolic reflector, Chem. Eng. Sci. 40 (1985) 2119–2127.
[36] O. Alfano, R. Romero, A. Cassano, A cylindrical photoreactor irradiated from the bottom-II. Models for the local volumetric rate of energy absorption with polychromatic radiation and their evaluation, Chem. Eng. Sci. 41 (1986) 1115–1116.
[37] O. Alfano, R. Romero, A. Negro, A. Cassano, A cylindrical photoreactor irradiated from the bottom-III. Measurement of absolute values of the local volumetric rate of energy absorption. Experiments with polychromatic radiation, Chem. Eng. Sci. 41 (1986) 1163–1169.
[38] L. Eary, J. Shramke, In: D. Melchior, R. Bassett (Eds.), Chemical Modeling of Aqueous Systems II; American Chemical Society Symposium Series 416, American Chemical Society, Washington, DC, 1990, pp. 379–396.
[39] Y. Lee, I.-K. Um, J. Yoon, Arsenic (III) oxidation by iron (VI) (ferrate) and subsequent removal of arsenic (V) by iron (III) coagulation, Environ. Sci. Technol. 37 (2003) 5750–5756.
[40] J. Cherry, A. Shaikh, D. Tallman, R. Nicholson, Arsenic species as an indicator of redox conditions in groundwater, J. Hydrol. 43 (1979) 373–392.
[41] M. Bissen, M.-M. Vieillard-Baron, A. Schindelin, F. Frimmel, TiO_2-catalyzed photooxidation of arsenite to arsenate in aqueous samples, Chemosphere 44 (2001) 751–757.
[42] H. Langner, C. Jackson, T. McDermott, W. Inskeep, Rapid oxidation of arsenite in a hot spring ecosystem, Yellowstone National Park, Environ. Sci. Technol. 35 (2001) 3302–3309.
[43] J. Wilkie, J. Hering, Rapid oxidation of geothermal arsenic (III) in stream waters of the eastern Sierra Nevada, Environ. Sci. Technol. 32 (1998) 657–662.